

Geophysical Research Letters

RESEARCH LETTER

10.1029/2020GL090677

Key Points:

- The impact of historical sea surface temperature trends in the North Atlantic since 1870 is simulated with a global atmospheric model
- Adjacent warming and cooling trends in the North Atlantic Ocean induce a negative NAO-like response and southward-shifted gyre forcing
- Propagation of planetary waves away from the North Atlantic induces a northward-shifted intertropical convergence zone in the Indian Ocean

Supporting Information:

- Figure S1

Correspondence to:

K. B. Karnauskas,
kristopher.karnauskas@colorado.edu

Citation:

Karnauskas, K. B., Zhang, L., & Amaya, D. J. (2021). The atmospheric response to North Atlantic SST trends, 1870–2019. *Geophysical Research Letters*, 48, e2020GL090677. <https://doi.org/10.1029/2020GL090677>

Received 4 SEP 2020

Accepted 12 DEC 2020

The Atmospheric Response to North Atlantic SST Trends, 1870–2019

Kristopher B. Karnauskas^{1,2} , Lei Zhang¹ , and Dillon J. Amaya² 

¹Department of Atmospheric and Oceanic Sciences, University of Colorado, Boulder, CO, USA, ²Cooperative Institute for Research in Environmental Sciences, University of Colorado, Boulder, CO, USA

Abstract Sea surface temperature (SST) observations in the North Atlantic since 1870 reveal a region of enhanced warming off the northeastern coast of North America, and a region of cooling to the south of Greenland. It has been hypothesized that these adjacent SST trends are a result of long-term changes in the buoyancy-driven ocean circulation—a slowdown of the Atlantic Meridional Overturning Circulation. The impacts of these historical SST trends on the atmosphere are estimated using idealized atmospheric general circulation model experiments in which the global atmosphere is exposed to modern climatological forcing minus the aforementioned regional SST trends. The local response includes a negative North Atlantic Oscillation tendency and southward shift of the wind forcing for the subtropical gyre. Due to planetary wave propagation, the regional SST trends also induce a northward shift of the intertropical convergence zone over the Indian Ocean. Implications for climate feedbacks and projections are discussed.

Plain Language Summary The ocean surface is warming over most of the planet, with a couple of notable exceptions. One is over the North Atlantic Ocean, just south of Greenland, where the temperature of the ocean surface has actually been cooling by about 1°C since 1870. Nearby, extending off the northeastern coastline of North America is a region where the ocean surface has been warming much faster than the global ocean on average—by about 1.5°C since 1870. This side-by-side pair of accelerated warming and cooling trends is likely due to a slowdown of the ocean's overturning circulation, which carries large amounts of heat energy from the tropics toward the poles. This paper reveals the effects of those unusual ocean temperature trends in the North Atlantic on the atmospheric circulation using a computer model of the global atmosphere. The model simulations indicate that these ocean temperature trends are causing shifts in the jet stream, changing the way the winds propel the upper ocean currents, and even have impacts quite far away by moving the tropical rain belt northward in the Indian Ocean.

1. Introduction

Many of the ways in which the atmospheric circulation has changed, and will change, in response to anthropogenic radiative forcing are a direct result of global energy imbalances. For example, the Hadley cells are expected to expand poleward due to perturbations in the global, zonal mean atmospheric energy budget (see Staten et al., 2020, and references therein). In the tropical Pacific, changes in the Walker circulation have been the subject of intense research, with a leading theory pointing to atmospheric thermodynamic constraints (e.g., Held & Soden, 2006; Vecchi et al., 2006; Vecchi & Soden, 2007). However, the Walker circulation is also strongly coupled to the underlying zonal sea surface temperature (SST) gradient (Bjerknes, 1969), which may influence trends in the Walker circulation itself (Clement et al., 1996; Heede et al., 2020; Xie et al., 2010). In contrast, other changes in atmospheric circulation may be forced from the bottom up—that is, driven by regional heterogeneities and gradients in the surface temperature response to anthropogenic forcing.

Of notable interest are SST trends emerging in instrumental records in the North Atlantic Ocean, which many studies have argued are due to changes in the buoyancy-driven ocean circulation—not driven by or coupled to surface wind forcing. In particular, warming much greater than the global mean SST trend (over 2°C since 1870) has been observed off the northeastern coast of North America (Figure 1a). This feature has been associated with recent marine heatwaves, generating substantial economic, and ecosystem impacts (Mills et al., 2013). Directly adjacent to this enhanced warming is a region just south of Greenland that has

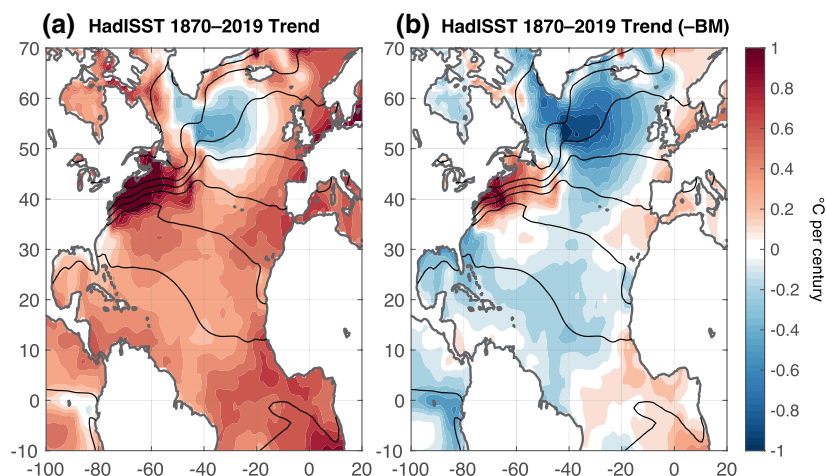


Figure 1. (a) Linear trend in monthly SST anomalies from 1870 to 2019 in HadISST observations ($^{\circ}\text{C}$ per century). (b) As in (a) but with the basin-wide median trend of 0.49°C per century (calculated from 55°S to 60°N) removed. Black contours in both panels represent the annual mean SST field from NOAA OIv2 observations (1982–2019), contoured every 4°C . All trends are significant at the 90% confidence level except where trends are very near zero (less than $\pm 0.1^{\circ}\text{C}$ per century) and in the far eastern equatorial Pacific Ocean. See Figure S1 for trends computed over different time periods, and Figure S2 for trends in seasonally averaged SST anomalies. SST, sea surface temperature.

cooled by approximately 0.75°C since 1870. This feature bucks the global mean warming trend, and has been dubbed the “Cold Blob” (or North Atlantic warming hole) in the scientific literature (e.g., Rahmstorf et al., 2015) and media. Relative to the Atlantic basin-wide median trend ($\sim 0.5^{\circ}\text{C}$ per century), both the enhanced warming and the Cold Blob trends have amplitude $\pm 1^{\circ}\text{C}$ per century (Figure 1b), representing an anomalous horizontal SST gradient of considerable magnitude. These patterns of SST change are closely related to concurrent patterns of sea level rise; Sallenger et al. (2012) showed that the rate of sea level rise along the northeastern U.S. coastline since 1950 is about four times greater than the global mean. Those tide-gauge based trends are confirmed by satellite altimeters and global, coupled climate models (Fasullo & Nerem, 2018; Yin et al., 2009).

It has been argued, and demonstrated using a range of global climate models, that both of the aforementioned long-term SST trends in the North Atlantic are a result of a weakening Atlantic Meridional Overturning Circulation (AMOC) in response to rising atmospheric CO_2 concentration (Caesar et al., 2018; Liu et al., 2020; Saba et al., 2016). In particular, while local forcing associated with internal atmospheric variability can superimpose short-term SST anomalies upon the long-term trend in this region (Chen et al., 2014, 2015), studies like Caesar et al. (2018) and Liu et al. (2020) showed that the pattern of warming and cooling described above emerges in coupled models as the spatial “fingerprint” of a weakening AMOC. The simulated AMOC weakening is consistent with a century-scale reconstruction in the Florida Current region (Piecuch, 2020), remote salinity trends (Zhu & Liu, 2020), and shorter-term circulation measurements at 26°N (Smeed et al., 2018), the latter of which have been linked directly to observed SST cooling south of Greenland via ocean heat transport calculations (Bryden et al., 2020).

Assuming that the observed SST trends in the North Atlantic (Figure 1) arise primarily from changes in large-scale ocean circulation unrelated to surface wind stress and heat flux, it is possible to quantify the atmospheric response to the aforementioned SST trends in a targeted modeling framework. In doing so, we would improve our understanding of the full response of the atmosphere to anthropogenic radiative forcing. In this study, we present a series of idealized atmospheric general circulation model (AGCM) experiments that are forced by the SST trends discussed above, which highlight both the local (i.e., within the North Atlantic basin) and remote atmospheric responses to these SST trends. It is important to note that these experiments are not an attempt to reproduce the total atmospheric response to climate change over the past century and a half; they are designed to isolate the response strictly to the regional SST trends in the North Atlantic. The model, model setup, and experiments are described in the following section. The

local and remote atmospheric responses are described in Section 3, and Section 4 provides a summary and discussion of the results relative to research highlighting responses not attributable to local North Atlantic SST forcing.

2. Model Setup and Experiments

The response of the global atmosphere to the regional SST trends discussed in the previous section was simulated using the Max Planck Institute (MPI) ECHAM4.6 model (Roeckner et al., 1996). ECHAM was integrated at T42 spectral horizontal resolution (corresponding to approximately 2.8° grid resolution) with 19 vertical levels. A total of four idealized experiments were conducted. The SST forcing in each experiment begins with a monthly climatology from the NOAA Optimal Interpolation version 2 (OIv2) (Reynolds et al., 2002) SST observations (originally 1° horizontal spatial resolution), averaged from 1982 to 2019. The first experiment, Exp1, is simply forced by the modern global SST climatology repeated 40 times, with all other forcings including carbon dioxide held constant at 1995 levels. The second experiment, Exp2, was conducted identically to Exp1 except that the cooling trend to the south of Greenland was subtracted from the modern climatology. The difference Exp1-Exp2 therefore represents the change over time due strictly to the cooling to the south of Greenland since the late 19th century but with a modern climatology everywhere else. Exp2 may be thought of as Earth today, except that the cooling never happened. Exp3 was conducted identically to Exp1 except that the warming trend off the northeastern coast of North America was removed from the modern climatology. Finally, Exp4 was conducted with both the cooling trend to the south of Greenland and the warming trend off the northeastern coast of North America subtracted from the modern climatology.

The two individual regional SST trends used to force the AGCM were obtained from observations as follows. First, the linear SST trend field, expressed in units °C per century, was computed using HadISST (Rayner et al., 2003) (1° resolution) from 1870 to 2019 (Figure 1a), and the basin-wide median trend (0.49 °C per century, calculated from 55°S–60°N) was removed (Figure 1b). A broad box was then defined around the cooling trend to the south of Greenland, and all grid cells with trend ≤ -0.25 °C per century retained (for Exp2). Similarly, a broad box was defined around the warming trend off the northeastern coast of North America, and all grid cells with trend ≥ 0.25 °C per century retained (for Exp3). The two SST anomaly patches, which do not overlap anywhere, were summed for Exp4. Finally, the anomaly fields were linearly interpolated to the T42 model grid. No changes were applied north of 60°N to avoid inadvertent modifications to the sea ice boundary conditions; a linear taper was applied across that line of latitude to avoid abrupt discontinuities in surface forcing. Comparing Figures 1b with 2c clearly indicates that the resulting SST forcings are reasonable reproductions of observed trends.

Exp4 may be considered the main experiment, since both trends emerge in the instrumental observations, while Exp2 and Exp3 enable more detailed diagnoses and attribution of the simulated atmospheric responses to the SST forcing as well as assessment of linearity in the responses to the individual SST anomalies. Throughout this paper, results labeled “Exp2” refer to Exp1-Exp2 differences, “Exp3” refers to Exp1-Exp3, and so on. The idealized AGCM experiments were conducted on a cluster with Intel Xeon E5-2620v2 processors using the MPI protocol for parallel processing. The first 4 years of each 40 years experiment were discarded as model spin-up, retaining 36 complete years for analysis. Since respective SST boundary conditions applied in each experiment were identical in each year of model integration, all interannual variability in the model solutions arises from internal atmospheric noise. There is negligible autocorrelation in such solutions; for example, one boreal summer is effectively independent of the next. This interannual variability is therefore leveraged to estimate the statistical significance of simulated differences in time-mean fields between the various experiments, for which we use a standard two-tailed Student's *t*-test where the effective number of degrees of freedom is in fact $N-1$. All relevant forcing and output fields are provided freely (see Data Availability Statement).

3. Results

3.1. Local Response

The atmospheric response within the North Atlantic sector to the prescribed SST anomalies is seasonally dependent (Figure 2), which is not surprising considering the large seasonality of the salient features of

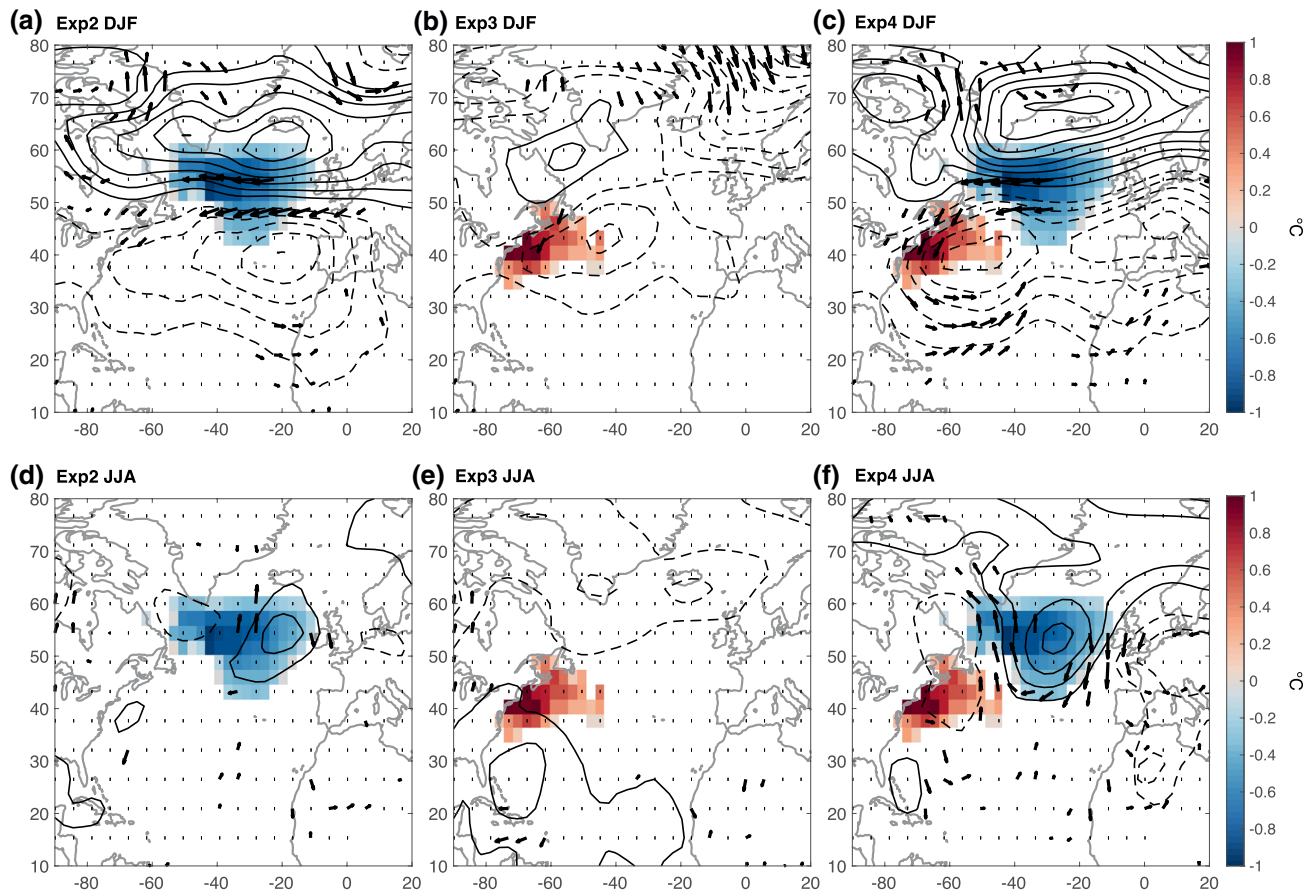


Figure 2. (a) Time-mean, boreal wintertime (DJF) SLP response (contoured every 0.25 mb, zero omitted) to the cold SST anomaly forcing shown in colors (Exp2, °C). Also shown are surface wind vector anomalies for which either vector component (zonal or meridional) is statistically significant at the 90% confidence level based on a two-tailed Student's *t*-test. (b) As in (a) but in response to the warm SST anomalies shown (Exp3). (c) As in (a) but in response to the cold and warm SST anomalies shown (Exp4). (d)–(f) as in (a)–(c) but for boreal summer (JJA). SST, sea surface temperature; SLP, sea level pressure.

the regional climatology including the Icelandic Low, Azores High, and midlatitude jet stream. In boreal winter (Figure 2a), the near-surface response to the cooling trend south of Greenland is characterized by a local deceleration of the midlatitude westerlies (manifest as anomalous easterlies directly over the cold anomaly), consistent with increased stability and reduced vertical mixing of eastward momentum in the free troposphere (Hayes et al., 1989; Wallace et al., 1989). The mass field adjusts toward geostrophic equilibrium with the zonal wind anomaly (Rossby, 1938), resulting in a roughly symmetric pair of sea level pressure (SLP) anomalies—an anticyclone to the north and a cyclone to the south (see also Figure S3a). The wintertime response to the warming trend is a low SLP anomaly centered over and extending eastward of the warm SST anomalies (Figure 2b). When the model is subject to both the cold and warm SST anomalies, the atmospheric response is an approximately linear superposition of the responses to the two individual SST anomalies (Figure 2c). There is a modest nonlinearity such that the simultaneous presence of both SST anomalies weakens the low SLP anomaly by ~20% and shifts the center of the high SLP anomaly northward by ~8° latitude (Figure S3b). The summertime response to the same SST forcing is dominated by the emergence of a high SLP anomaly over the cold patch (Figures 2d–2f). In comparison, the local summertime response is muted and relatively unremarkable, save for potential impacts on seasonal sea ice retreat that are not modeled in this framework; the remainder of this paper will focus on the boreal wintertime response.

The wintertime response over the North Atlantic to the observed regional SST trends (Figure 2c) bears striking resemblance to the negative phase of the North Atlantic Oscillation (NAO). For consistency, the NAO was defined in the model by calculating the leading empirical orthogonal function (EOF) of wintertime

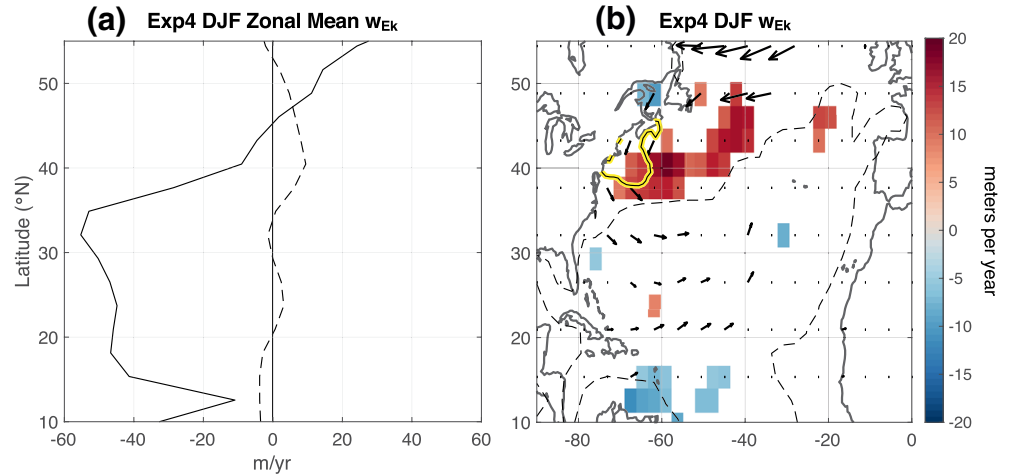


Figure 3. (a) Solid: Zonal mean (70°W–15°W), time-mean, boreal wintertime (DJF) Ekman pumping velocity (w_{Ek} , solid line, m/yr , positive upward) from the control experiment (Exp1). Dashed: As in solid but the w_{Ek} response to cold and warm SST anomalies (i.e., Exp4). (b) Colors: Time-mean, boreal wintertime (DJF) w_{Ek} response (m/yr) to cold and warm SST anomalies (i.e., Exp4), only showing values statistically significant at the 90% confidence interval based on a two-tailed Student's t -test. The dashed contour indicates the -30 m/yr (downward) w_{Ek} isopleth to approximately outline the region of wind forcing for the subtropical gyre. The yellow contour outlines the region where the observed SST trend is at least 0.75°C per century. Also shown are surface wind stress anomalies for which either vector component (zonal or meridional) is statistically significant at the 90% confidence level based on a two-tailed Student's t -test. SST, sea surface temperature.

(DJF) SLP variability in the North Atlantic (Hurrell, 1995). The SLP response indeed projects very strongly onto the simulated NAO (Figure S4); the spatial correlation coefficient between the SLP response and the NAO pattern is -0.94 . The implications of this result are discussed in the following section.

While there is, of course, no interactive ocean in our AGCM framework, implications for some key atmospheric drivers of ocean circulation can be gleaned from the model solutions. Specifically, the surface wind anomalies evident in Figure 2c are quite relevant to the wind forcing of the subtropical ocean gyre. To characterize the anomalous wind forcing of the ocean, the Ekman pumping velocity (w_{Ek}) was calculated as:

$$w_{Ek} = \nabla \times \frac{\bar{\tau}}{\rho f} \quad (1)$$

where $\bar{\tau}$ is the wind stress vector, ρ is the seawater density, and f is the Coriolis parameter. The subtropical gyre is fundamentally driven by downward Ekman pumping velocity ($w_{Ek} < 0$), as induced by negative wind stress curl ($\nabla \times \bar{\tau} < 0$) in the Northern Hemisphere. The resulting depression of the thermocline near the center of the basin is mirrored by a relative maximum of dynamic sea surface height, about which geostrophic currents flow clockwise.

The simulated response of surface winds over the North Atlantic to the regional SST trends is equivalent to a southward shift of the region of negative wind stress curl and diagnosed Ekman pumping velocity (Figure 3). Along the poleward edge of climatological Ekman pumping, a positive wind stress curl about the low SLP anomaly induces anomalous Ekman suction ($w_{Ek} > 0$). Along the equatorward edge of climatological Ekman pumping, a negative wind stress curl due to a positive meridional gradient of zonal wind stress ($\partial \tau_x / \partial y > 0$) south of the cyclonic response induces further Ekman pumping. Both of these Ekman pumping responses are particularly significant in the western half of the basin. Overall, there is an equatorward shift of the region of Ekman pumping without a significant change in magnitude. The Ekman suction anomaly along the eastern periphery of the enhanced warming trend (Figure 3b), by order-of-magnitude estimate of the anomalous vertical temperature advection term $-w_{Ek} \Delta T/h$ (where $w_{Ek} = \sim 10 \text{ m/yr}$, $\Delta T = 0.1^\circ\text{C}$ for the temperature jump across the base of the mixed layer, and $h = 100 \text{ m}$ for wintertime mixed layer depth), would induce an SST tendency of order -1°C per century; implications are discussed in section 4.

3.2. Remote Response

In response to SST anomalies of order 1°C in the midlatitudes, local perturbations to the jet stream and propagation of planetary waves lead to some robust responses across the global atmosphere. The surface pressure anomalies discussed previously extend well throughout the troposphere and, by geostrophy, lead to a deceleration (acceleration) along the northern (southern) flank of the midlatitude jet stream, ultimately manifesting as a slight southward shift of the jet (Figures 4a and 4b). The southward-shifted jet brings wetter conditions (~20% increase in precipitation) to southern Europe (Figure 4c), consistent with the negative phase of the NAO.

Further afield, there is a significant climate response in the tropical Indian Ocean. The prescribed SST perturbations in the North Atlantic lead to the setup of a teleconnection pattern that forces an anomalous meridional, cross-equatorial SLP gradient there (Figures 4b–4d). Horizontal stationary Rossby wave flux, calculated according to Plumb (1985; see Equation 4.9), establishes the direct link between the anticyclone in the North Atlantic and the cyclone over the Arabia Sea and India (Figure 4b), which is manifest as a low SLP anomaly at the surface. The resulting anomalous meridional SLP gradient in the Indian Ocean drives a northward surface wind anomaly that weakens the Asian-Australian winter monsoon, shifting northward the location of convergence, and hence the ITCZ and precipitation maximum also shift northward (Figures 4c and 4d). The northward shift of the Indian Ocean ITCZ is particularly robust in boreal winter, but is present year-round (Figures S5d and S6).

4. Summary and Discussion

This paper presents a set of global atmospheric model experiments with prescribed patches of anomalous SST forcing in the North Atlantic mimicking the observed, historical trends since the late nineteenth century. Within the North Atlantic sector, the time-mean, boreal wintertime response strongly projects onto the negative phase of the NAO, both in terms of modulating the salient features of the seasonal mean climate and presentation of impacts. Interestingly, previous research has identified a trend toward the positive phase of the NAO in historical observations (Hurrell, 1995; Hurrell et al., 2004), which has been attributed to progressive warming of the tropical Indian Ocean (Hoerling et al., 2004). Results presented herein suggest that the ongoing regional SST trends in the North Atlantic may be damping that response.

These results also raise the possibility of several potential feedbacks in the real, coupled world. The positive Ekman pumping velocity anomaly over the North Atlantic, in response to the prescribed SST trends, would introduce a negative feedback on the enhanced warming off the coast of North America. The wind stress curl induced by the prescribed SST trends would therefore damp the warming along the eastern edge of the region of enhanced warming, contributing to its appearance as a coastal feature. It is also conceivable that the weakened westerlies over (and in response to) the cooling trend south of Greenland would introduce a local negative feedback through reduced turbulent heat flux, in line with Hu and Fedorov (2019).

An important aspect of the local response is a southward shift of the wind forcing of the subtropical ocean gyre. A tendency for an equatorward-shifted subtropical gyre including the Gulf Stream might, in a simple view, advect warmer water poleward along the western boundary (given origins deeper into the tropics), while not transporting heat as *far* poleward (given an abbreviated poleward reach). Such alterations to meridional heat transport would tend to warm SST somewhere along the path of the western boundary current, and cool SST near its poleward limit—aptly describing the SST trends constituting the forcing in these experiments. It is therefore plausible that the local atmospheric response to the observed regional SST trends introduces a positive feedback to the SST trends. In coupled models and in the real world, cause, effect, and feedback become quite ambiguous; for example, studies that have previously attributed the North Atlantic regional SST trends prescribed in these experiments to a slowdown of the AMOC also exhibited a *northward* shift of the Gulf Stream (Caesar et al., 2018; Saba et al., 2016). Again, these experiments are not intended to reproduce the *total* response of the climate system to anthropogenic radiative forcing—only that which is attributable specifically to the emergence of these regional SST anomalies.

Finally, the simulated northward shift of the Indian Ocean ITCZ adds to a growing body of research highlighting the importance of interactions between ocean basins, although the overwhelming focus thus far

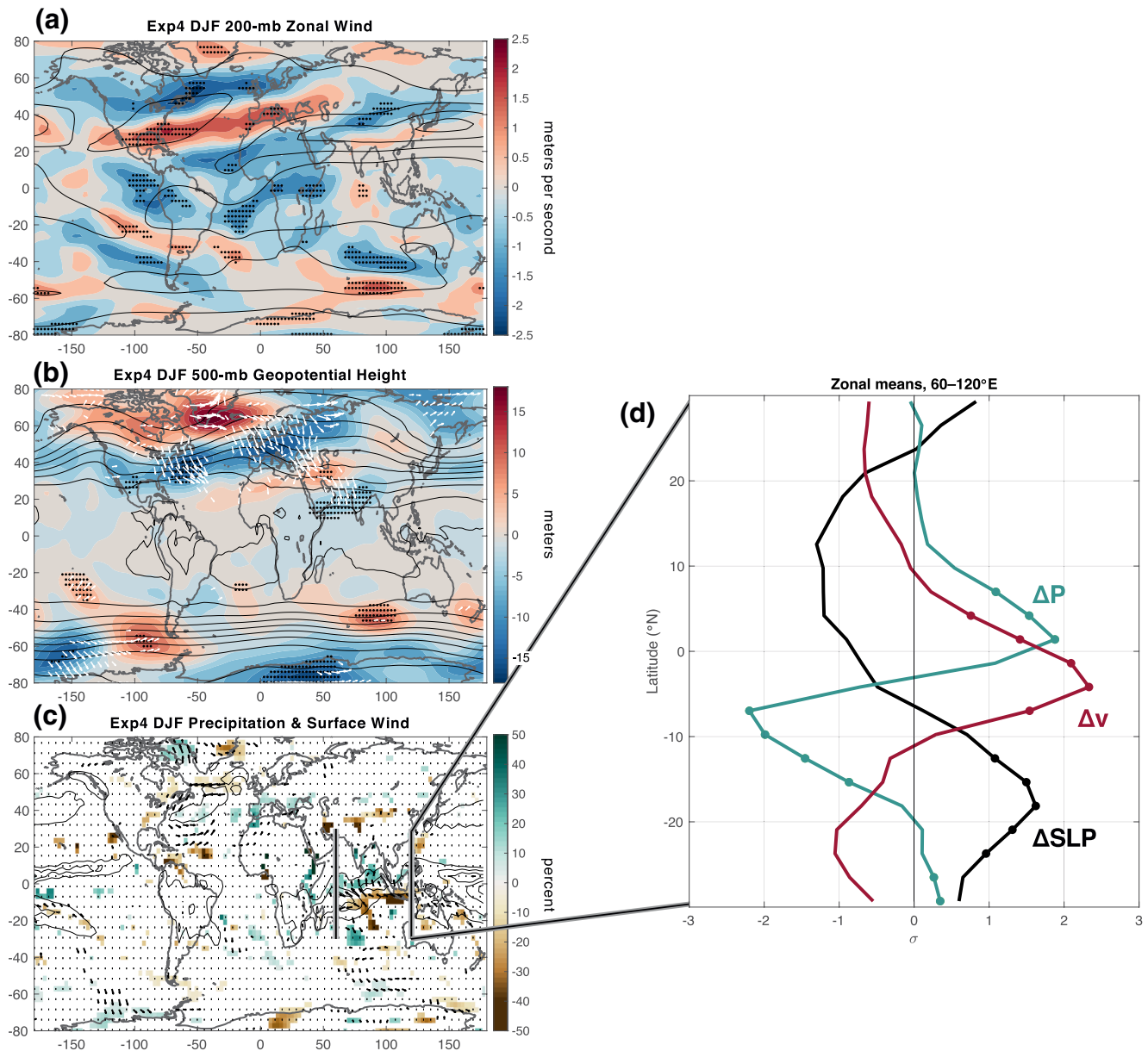


Figure 4. Global, time-mean, boreal wintertime (DJF) responses to cold and warm SST anomalies in the North Atlantic (i.e., Exp4). (a) 200-mb zonal wind response (colors, m/s) and control (Exp1) mean DJF climatology (contours, every 20 m/s starting at ± 10 m/s). (b) 500-mb geopotential height response (colors, m) and Exp1 climatology (contours, every 100 m), and horizontal stationary wave flux (white vectors). (c) Precipitation response (colors, %), surface wind response (vectors), and Exp1 climatology (contours, every 5 mm/day, zero omitted). In (a) and (b), responses where the difference is statistically significant at the 90% confidence interval based on a two-tailed Student's *t*-test are stippled. In (c), only significant values are shown. (d) Responses of SLP (black), surface meridional wind (red), and precipitation (blue) within the tropical Indian Ocean to cold and warm SST anomalies (i.e., Exp4), zonally averaged from 60°E–120°E. Latitudes at which the difference between zonally averaged profiles is statistically significant are marked with filled circles. To facilitate visual comparison, profiles in (d) are normalized by their standard deviation over the latitude domain shown. See Figure S5 for the equivalent fields (a)–(c) for boreal summertime (JJA). SST, sea surface temperature; SLP, sea level pressure.

has been between tropical ocean basins (Cai et al., 2019). The stationary Rossby wave train mechanism evident in these simulations is similar to that recently shown to be responsible for a North Atlantic–Siberian teleconnection on decadal time scales (Nicoli et al., 2020; Sun et al., 2015). While Hoerling et al. (2004) and Hu and Fedorov (2019, 2020) have shown that the tropical Indian Ocean can influence North Atlantic climate, these experiments hint that such interbasin interactions can go both ways and on similar (quasi steady) time scales.

In observations, it may prove challenging to detect the presence of the simulated responses shown here due to the cacophony of internal atmospheric noise, coupled climate variability, and other externally forced responses. However, this challenge does not render them *absent* from the real world and observational records—particularly since both the local and remote responses arise through relatively intuitive application of basic atmospheric dynamics. In reality, the atmospheric responses to North Atlantic SST trends likely contribute to the totality of historical climate change, and the scale of their feedbacks could magnify under future radiative forcing so long as the SST trends in the North Atlantic continue to progress. Advances on this front would benefit from the application of additional techniques such as coupled models (i.e., pacemaker style experiments), a comparison across different atmospheric models (e.g., AMIP style experiments), and models with higher atmospheric resolution.

Data Availability Statement

All observational data sets used in this study are publicly available. The NOAA OI v2 data set is available at <https://psl.noaa.gov/data/gridded/data.noaa.oisst.v2.html>. The HadISST data set is available at <https://www.metoffice.gov.uk/hadobs/hadisst/>. All relevant forcing and output fields from the AGCM experiments are provided at <https://www.colorado.edu/oclab/arnast>.

Acknowledgments

The authors thank Yu Kosaka for valuable discussion, and funding from the CIRES Visiting Fellows Program (DJA) and the NASA Sea Level Change Science Program, Award 80NSSC20K1123 (KBK).

References

- Bjerknes, J. (1969). Atmospheric teleconnections from the equatorial Pacific. *Monthly Weather Review*, 97, 163–172.
- Bryden, H. L., Johns, W. E., King, B. A., McCarthy, G., McDonagh, E. L., Moat, B. I., & Smeed, D. A. (2020). Reduction in ocean heat transport at 26°N since 2008 cools the eastern subpolar gyre of the North Atlantic Ocean. *Journal of Climate*, 33, 1677–1689.
- Caesar, L., Rahmstorf, S., Robinson, A., Feulner, G., & Saba, V. (2018). Observed fingerprint of a weakening Atlantic Ocean overturning circulation. *Nature*, 556, 191–196.
- Cai, W., Wu, L., Lengaigne, M., Li, T., McGregor, S., Kug, J.-S., et al. (2019). Pan-tropical climate interactions. *Science*, 363, 1–11.
- Chen, K., Gawarkiewicz, G., Kwon, Y.-O., & Zhang, W. G. (2015). The role of atmospheric forcing versus ocean advection during the extreme warming of the Northeast U.S. continental shelf in 2012. *Journal of Geophysical Research: Oceans*, 120, 4324–4339. <https://doi.org/10.1002/2014JC010547>
- Chen, K., Gawarkiewicz, G. G., Lentz, S. J., & Bane, J. M. (2014). Diagnosing the warming of the Northeastern U.S. Coastal Ocean in 2012: A linkage between the atmospheric jet stream variability and ocean response. *Journal of Geophysical Research: Oceans*, 119, 218–227. <https://doi.org/10.1002/2013JC009393>
- Clement, A. C., Seager, R., Cane, M. A., & Zebiak, S. E. (1996). An ocean dynamical thermostat. *Journal of Climate*, 9, 2190–2196.
- Fasullo, J. T., & Nerem, R. S. (2018). Altimeter-era emergence of the patterns of forced sea-level rise in climate models and implications for the future. *Proceedings of the National Academy of Sciences of the United States of America*, 115, 12944–12949.
- Hayes, S., McPhaden, M., & Wallace, J. (1989). The influence of sea-surface temperature on surface wind in the eastern equatorial Pacific: Weekly to monthly variability. *Journal of Climate*, 2, 1500–1506.
- Heede, U. K., Fedorov, A. V., & Burls, N. J. (2020). Time scales and mechanisms for the tropical Pacific response to global warming: A tug of war between the ocean thermostat and weaker walker. *Journal of Climate*, 33, 6101–6118.
- Held, I. M., & Soden, B. J. (2006). Robust responses of the hydrological cycle to global warming. *Journal of Climate*, 19, 5686–5699.
- Hoerling, M. P., Hurrell, J. W., Xu, T., Bates, G. T., & Phillips, A. S. (2004). Twentieth century North Atlantic climate change. Part II: Understanding the effect of Indian Ocean warming. *Climate Dynamics*, 23, 391–405.
- Hu, S., & Fedorov, A. V. (2019). Indian Ocean warming can strengthen the Atlantic meridional overturning circulation. *Nature Climate Change*, 9, 747–751.
- Hu, S., & Fedorov, A. V. (2020). Indian Ocean warming as a driver of the North Atlantic warming hole. *Nature Communications*, 11, 4785.
- Hurrell, J. W. (1995). Decadal trends in the North Atlantic oscillation: Regional temperatures and precipitation. *Science*, 269, 676–679.
- Hurrell, J. W., Hoerling, M. P., Phillips, A. S., & Xu, T. (2004). Twentieth century north Atlantic climate change. Part I: Assessing determinism. *Climate Dynamics*, 23, 371–389.
- Liu, W., Fedorov, A. V., Xie, S.-P., & Hu, S. (2020). Climate impacts of a weakened Atlantic Meridional Overturning Circulation in a warming climate. *Science Advances*, 6, eaaz4876.
- Mills, K. E., Pershing, A. J., Brown, C. J., Chen, Y., Chiang, F.-S., Holland, D. S., et al. (2013). Fisheries management in a changing climate: Lessons from the 2012 ocean heat wave in the Northwest Atlantic. *Oceanography*, 26, 191–195.
- Nicoli, D., Bellucci, A., Iovino, D., Ruggieri, P., & Gualdi, S. (2020). The impact of the AMV on Eurasian summer hydrological cycle. *Scientific Reports*, 10, 14444.
- Piecuch, C. G. (2020). Likely weakening of the Florida Current during the past century revealed by sea-level observations. *Nature Communications*, 11, 3973.
- Plumb, R. A. (1985). On the three-dimensional propagation of stationary waves. *Journal of the Atmospheric Sciences*, 42, 217–229.
- Rahmstorf, S., Box, J., Feulner, G., Mann, M. E., Robinson, A., Rutherford, S., & Schaffernicht, E. J. (2015). Exceptional twentieth-century slowdown in Atlantic Ocean overturning circulation. *Nature Climate Change*, 5, 475–480.
- Rayner, N. A., Parker, D. E., Horton, E. B., Folland, C. K., Alexander, L. V., Rowell, D. P., et al. (2003). Global analyses of sea surface temperature, sea ice, and night marine air temperature since the late nineteenth century. *Journal of Geophysical Research*, 108(D14), 4407. <https://doi.org/10.1029/2002JD002670>
- Reynolds, R. W., Rayner, N. A., Smith, T. M., Stokes, D. C., & Wang, W. (2002). An improved in situ and satellite SST analysis for climate. *Journal of Climate*, 15, 1609–1625.

- Roeckner, E., Arpe, K., Bengtsson, L., Christoph, M., Claussen, M., Dümenil, L., et al. (1996). *The atmospheric general circulation Model ECHAM-4: Model description and simulation of present-day climate* (Tech. Rep. 218, pp. 90). Hamburg, Germany: Max-Planck-Institut für Meteorologie.
- Rossby, C.-G. (1938). On the mutual adjustment of pressure and velocity distributions in certain simple current system, II. *Journal of Marine Research*, 1, 239.
- Saba, V. S., Griffies, S. M., Anderson, W. G., Winton, M., Alexander, M. A., Delworth, T. L., et al. (2016). Enhanced warming of the Northwest Atlantic Ocean under climate change. *Journal of Geophysical Research: Oceans*, 121, 118–132. <https://doi.org/10.1002/2015JC011346>
- Sallenger, A., Doran, K., & Howd, P. (2012). Hotspot of accelerated sea-level rise on the Atlantic coast of North America. *Nature Climate Change*, 2, 884–888.
- Smeed, D. A., Josey, S. A., Beaulieu, C., Johns, W. E., Moat, B. I., Frajka-Williams, E., et al. (2018). The North Atlantic Ocean is in a state of reduced overturning. *Geophysical Research Letters*, 45, 1527–1533. <https://doi.org/10.1002/2017GL076350>
- Staten, P. W., Grise, K. M., Davis, S. M., Karneuskas, K. B., Waugh, D. W., Maycock, A., et al. (2020). Tropical widening: From global variations to regional impacts. *Bulletin of the American Meteorological Society*, 101, E897–E904.
- Sun, C., Li, J., & Zhao, S. (2015). Remote influence of Atlantic multidecadal variability on Siberian warm season precipitation. *Scientific Reports*, 5, 16853.
- Vecchi, G. A., & Soden, B. J. (2007). Global warming and the weakening of the tropical circulation. *Journal of Climate*, 20, 4316–4340.
- Vecchi, G., Soden, B., Wittenberg, A., Held, I. M., Leetmaa, A., & Harrison, M. J. (2006). Weakening of tropical Pacific atmospheric circulation due to anthropogenic forcing. *Nature*, 441, 73–76.
- Wallace, J., Mitchell, T., & Deser, C. (1989). The influence of sea-surface temperature on surface wind in the eastern equatorial Pacific: Seasonal and interannual variability. *Journal of Climate*, 2, 1492–1499.
- Xie, S. P., Deser, C., Vecchi, G. A., Ma, J., Teng, H., & Wittenberg, A. T. (2010). Global warming pattern formation: Sea surface temperature and rainfall. *Journal of Climate*, 23, 966–986.
- Yin, J., Schlesinger, M., & Stouffer, R. (2009). Model projections of rapid sea-level rise on the northeast coast of the United States. *Nature Geoscience*, 2, 262–266.
- Zhu, C., & Liu, Z. (2020). Weakening Atlantic overturning circulation causes South Atlantic salinity pile-up. *Nature Climate Change*, 10, 998–1003.